Localized anisotropic tomography with well information in VTI media

Andrey Bakulin, Marta Woodward, Dave Nichols, Konstantin Osypov, Olga Zdraveva,*
WesternGeco/Schlumberger

Summary

We outline a concept of localized seismic tomography constrained by well information and apply it to building vertically transversely isotropic (VTI) velocity models in depth. We localize tomography to a limited volume around the well and eliminate non-uniqueness by supplementing surface seismic data with the well information. Finally, we regularize tomography with smoothness or any reasonable a priori information constraints. As a result we recover the anisotropic velocity field around the well. We present a synthetic data example of anisotropic tomography applied to a 1D VTI model. We demonstrate three different cases of introducing additional information. In the first case vertical velocity is known and tomography inverts for Thomsen's ε and δ profiles. In the second case, tomography simultaneously inverts for all three VTI parameters including vertical velocity using a joint dataset that consists of surface seismic data and vertical checkshot traveltimes. In the third case seismic data and depth markers are used to invert for all three Thomsen parameters. Localized tomography confidently recovers correct global vertical profiles of anisotropic velocity field along the entire well length of 11 km. Anisotropic tomography with well constraints has multiple advantages over manual approaches and deserves a place in the portfolio of model-building tools.

Introduction

Anisotropic depth imaging continues to gain popularity and vertical transverse isotropy (VTI) has become a default model type for depth imaging. This progression from isotropy to anisotropy has been driven by increasingly stringent requirements on image positioning errors in true geological depth. However, anisotropic parameter estimation is known to be a highly non-unique process, even for layered geological environments (Grechka et al., 2002). While many different depth models may flatten seismic gathers, only one of them gives the correct depth positioning. A practical solution to this problem is to inject well measurements and all possible a priori information to constrain the anisotropic models (Bear et al., 2005). In this study we introduce a notion of localized anisotropic tomography with well information and show that it may recover the correct anisotropic velocity field in the vicinity of the well in an automated fashion.

Anisotropic tomography with well constraints

Reflection tomography (Woodward et al., 2008) has become a workhorse of velocity-model building for depth imaging. Anisotropic extensions of tomography were reported for VTI and TTI media (Zhou et al., 2004; Woodward et al., 2008); however, non-uniqueness makes it difficult to use. Blind use of anisotropic tomography may lead to velocity/anisotropy fields that flatten the gathers and yet are geologically implausible. The practical solution is to supplement reflection data with additional information coming from wells. Since well data is inherently local, it makes sense to perform joint inversion of seismic and well data but only in the vicinity of the well. The aim is to derive a localized anisotropic velocity model that is consistent with well and other data. Smoothness and other constraints are imposed to avoid artifacts, although more sophisticated geological constraints may also be incorporated. While one may intervene and edit the model at any step of the process, the aim of interactive tomography is to deliver a constrained solution in an automated fashion.

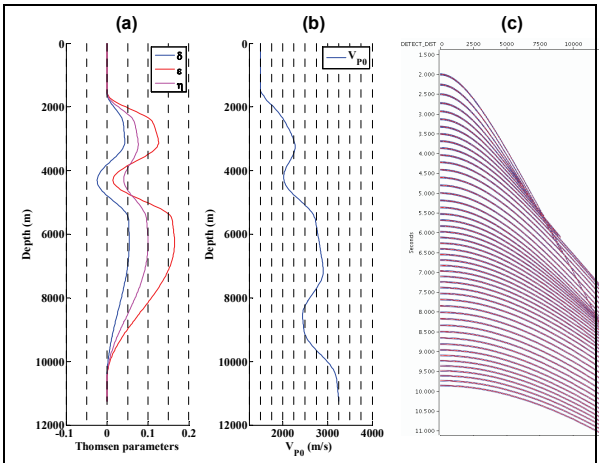

Figure 1: Deepwater 1D VTI model used for tomography: a) anisotropic parameters, b) vertical velocity, c) prestack gather. Water depth is at 1500 m..

Synthetic examples

Let us apply anisotropic tomography with well constraints to a simple deepwater model (Figure 1). The subsurface is represented by horizontally layered VTI sediment. The model has smooth vertical variation of velocity and anisotropy (Figure 1a, b). Two pronounced velocity inversions are present in the model. A cable length of 12 km is assumed. A prestack gather computed with anisotropic ray tracing is shown in Figure 1c. Reflected events from 49 interfaces of density contrast are located every 200 m.

It is known that for this type of model geometry long-spread reflection data may constrain only two parameters:

$V_{NMO} = V_{P0}\sqrt{1+2\delta}$ is constrained by short-spread moveout, whereas $\eta \approx \varepsilon - \delta$ can be estimated from a long-offset moveout. Here V_{P0}, ε, and δ are the three independent Thomsen parameters that completely describe VTI velocity field whereas η is a derivative parameter useful for analysis. If no well information is available then seismic data can be imaged with a series of equivalent models that preserve $V_{NMO} = V_{P0}\sqrt{1+2\delta}$ and η, but have different V_{P0}, ε, δ. In order to recover a true model, we need to provide additional constraints to the tomography. Here we examine three possible scenarios of localized tomography with well constraints:

- fix the vertical velocity field to correct values and invert surface seismic data for anisotropy parameters ε and δ
- jointly invert surface seismic and vertical checkshot data for three parameters: V_{P0}, ε, δ
- jointly invert surface seismic and a set of depth markers for three parameters: V_{P0}, ε, δ.

We utilize the Westerngeco reflection tomography workflow described by Woodward et al (2008). In all cases, we assume isotropic initial model, although in real life we would likely start with the regional non-zero anisotropic profiles which are expected to be closer to the desired true model.

Two-parameter inversion after fixing vertical velocity

In this scenario we assume that vertical velocity V_{P0} was estimated from acoustic logs or checkshot. Thus tomography is given a true vertical velocity field and is tasked to perform simultaneous inversion for Thomsen's δ and ε using all available offsets. To avoid small-scale artifacts and to prevent any potential instabilities, we used a conservative scheme for the smoothness constraints. For the first two iterations we opted to recover the smoothest part of the anisotropy profile (Figure 2). The third and forth iterations were allowed to alter the anisotropy profile at a finer scale and they promptly recovered actual highs and lows. After the last iteration, the standard deviation of Thomsen's ε and δ from their true values are 0.006 and 0.011, respectively, across the entire well depth of 11 km.

Three-parameter inversion of seismic and checkshot

In a second scenario we invert simultaneously for three VTI parameters (V_{P0}, ε, δ) using joint tomographic inversion of vertical checkshot traveltimes and surface seismic data. Thus cost function has contributions from each data type. The checkshot consists of 191 observations recorded over the depth range from 1.5 km to 11 km. Since the checkshot misfit has far fewer data points compared to the seismic residual moveout observations, it was weighted to ensure that tomography treats VSP and seismic on equal footing. Figure 3a shows that the starting model has too fast vertical velocity and the checkshot misfit reaches 80 ms. Already after the first iteration the maximum misfit reduces to less than 10 ms (Figure 3b). After the final fourth iteration we observe zero-mean checkshot errors that are less than 1.5 ms which is reasonable from a standpoint of the possible measurement error (~1ms) as well as fact that we find best smooth model that fits the data. After the last iteration (Figure 4), the standard deviation of Thomsen's ε and δ from their true values are 0.008 and 0.013, respectively, across the entire well depth of 11 km, which is slightly less accurate then in the previous example.

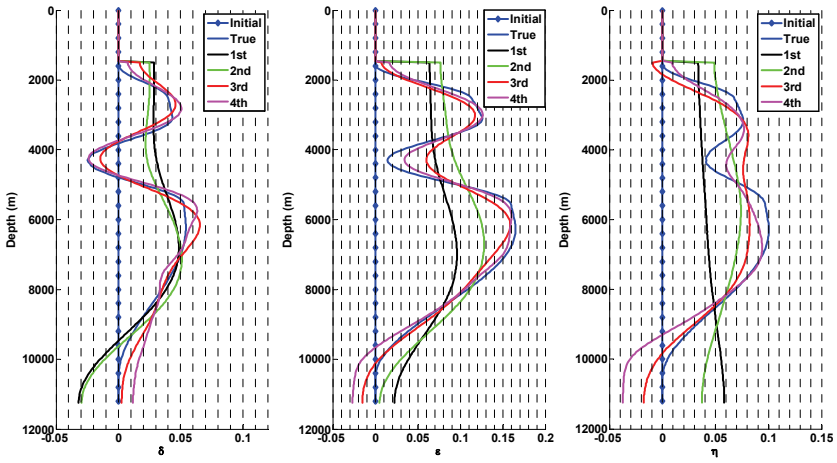

Figure 2: Convergence of two-parameter anisotropic inversion after fixing vertical velocity. Anisotropy profiles after each iteration are shown together with initial (zero) and true models.

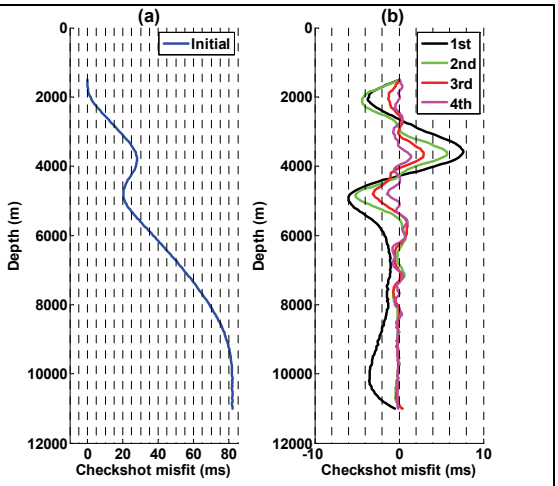

Figure 3: Misfit in checkshot traveltimes for initial model (a) and all subsequent tomography iterations (b). Misfit is computed as a difference between measured and predicted traveltimes.

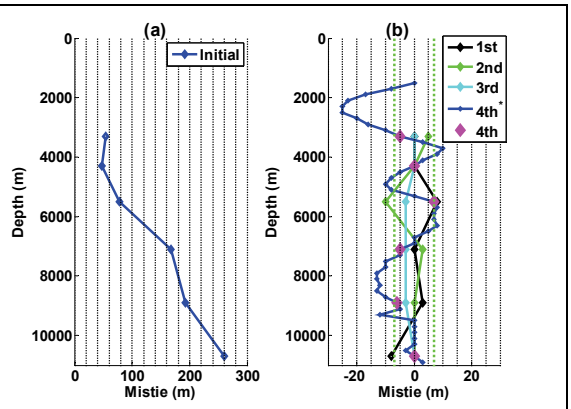

Figure 5: Mistie for initial model (a) and all subsequent tomography iterations (b). After last iteration all misties used by tomography are less than 7 m (b). Note that while depth mismatch for events used by tomography are small [magenta diamonds or 4th on b)], misties for other events can reach up to 25 m [blue diamonds or 4th* on b)].

Three-parameter inversion of seismic and markers

In a third scenario well data consists of six depth markers which are shown for the initial model in Figure 5a. Tomography inverts for three Thomsen parameters using a joint dataset consisting of seismic and well-depth misties. As in the VSP case, markers need to be given sufficient weight in the cost function to ensure that tomography simultaneously flattens the image gathers and eliminates the misties. Figure 5b shows that tomography efficiently reduces the misties by adjusting the vertical velocity while simultaneously flattening the gathers by aggressively updating anisotropy parameters (Figure 6). After four iterations, tomography accomplishes the goal of making all the image gathers flat while minimizing the misties to less than 7 m. However, only an approximation to the true model is recovered due to the velocity-depth ambiguity that exists between the marker points (Figure 6). As a result misties for the events that did not participate in tomography may remain noticeable. For example misties above the first marker are up to 25 m (Figure 5b). Due to interplay between all three VTI parameters, errors in velocity result in less accurate estimation of ε and δ in particular above the first marker. Such artifacts were not present in the previous example with a checkshot since velocity was constrained by 191 depth points across the entire sediment section instead of six sparse marker locations in this case. Nevertheless, the recovered estimate is a reasonable approximation to an actual VTI model. In order to remove geologically implausible jumps in anisotropy parameters at the water bottom, one can either edit the top portion of anisotropic profiles (with corresponding velocity update) or introduce additional tapering constraints into the tomography.

Conclusions

We presented a concept of anisotropic tomography with well constraints. We have demonstrated that by localizing the tomography to the volume near the well and by introducing proper constraints from the well, we can eliminate or reduce non-uniqueness and recover a good estimate of Thomsen parameters and velocity around the well. We presented three practical scenarios where well data is introduced either by fixing vertical velocity, by providing vertical checkshot traveltimes, or by introducing depth markers. In all three cases a good approximation to an actual VTI velocity field is easily recovered. Accuracy of the recovered field is controlled by the amount of well data: best reconstruction is achieved with correct and fixed vertical velocity. Slightly less accurate is reconstruction with dense vertical checkshot traveltimes, whereas the largest discrepancies between the recovered and the true VTI velocity field are observed for the third case of sparse depth markers. Interactive tomography may replace the currently used anisotropic calibration approach that uses manual layer-stripping 1D inversion or it can be used as a good starting guess for a manual refinement. We anticipate that this approach of well-constrained tomography can be applied to inversion for anisotropy in 2D and 3D models and would allow anisotropic calibration with deviated wells.

Acknowledgements

We thank Dmitry Alexandrov (summer intern from St. Petersburg State University) for help with generating the synthetic dataset.

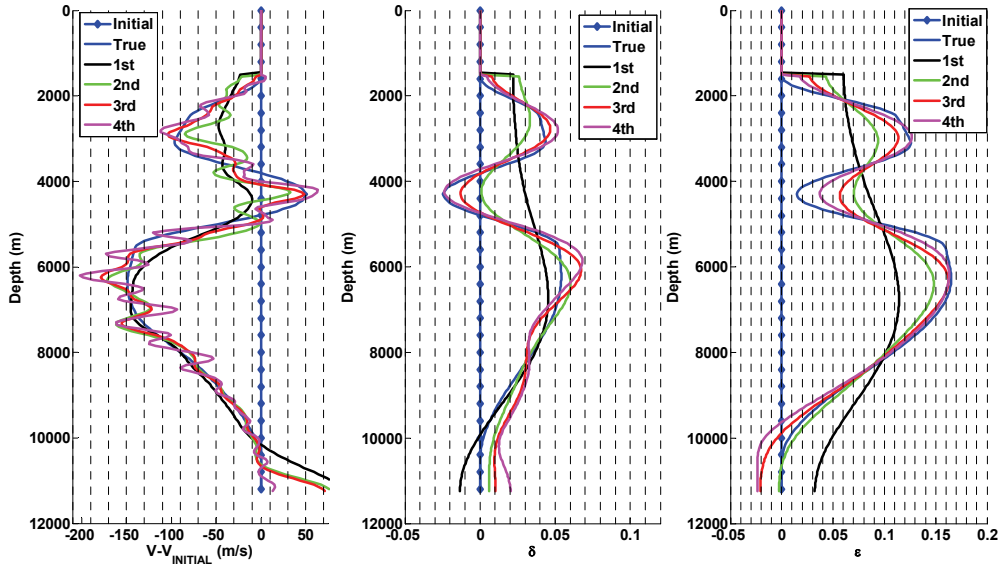

Figure 4: Convergence of three-parameter anisotropic inversion of seismic and checkshot data. Velocity and anisotropy profiles after each iteration are shown together with initial and true models.Velocity is shown as the difference between current velocity at each iteration and the initial velocity profile.

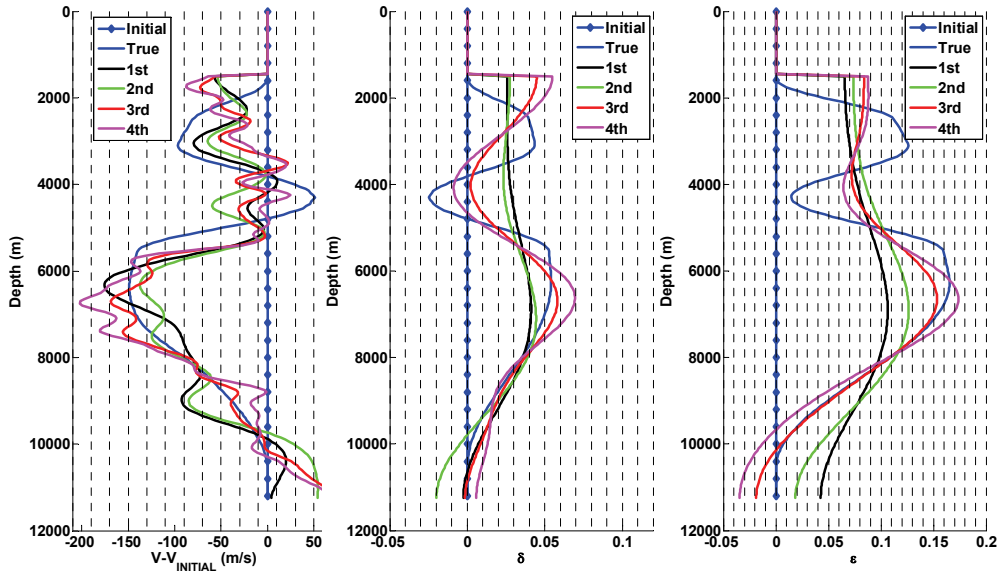

Figure 6: Convergence of three-parameter anisotropic inversion of seismic and marker data. Velocity and anisotropy profiles after each iteration are shown together with initial and true models.Velocity is shown as the difference between current velocity at each iteration and the initial velocity profile.

EDITED REFERENCES

Note: This reference list is a copy-edited version of the reference list submitted by the author. Reference lists for the 2009 SEG Technical Program Expanded Abstracts have been copy edited so that references provided with the online metadata for each paper will achieve a high degree of linking to cited sources that appear on the Web.

REFERENCES

Bear, L. K., T. A. Dickens, J. R. Krebs, J. Liu, and P. Traynin, 2005, Integrated velocity model estimation for improved positioning with anisotropic PSDM: The Leading Edge, **24**, 622–634.

Grechka, V, Tsvankin, I, Bakulin, A., Hansen, J. O. and Signer, C., 2002, Joint inversion of PP and PS reflection data for VTI media: A North Sea case study: Geophysics, **67**, 1382–1395.

Woodward, M., Nichols, D., Zdraveva, O., Whitfield, P., Johns, T., 2008, A decade of tomography: Geophysics, **73**, no. 5, VE5–VE11.

Zhou, H., D. Pham, S. Gray, and B. Wang, 2004, Tomographic velocity analysis in strongly anisotropic TTI media: 74th Annual International Meeting, SEG, Expanded Abstracts, 2347–2350.